

Supporting Information

Longitudinally Expanded Ni-Based Metal-Organic Framework with Enhanced Double Nickel Cation Catalysis Reaction Channels for Non-Enzymatic Sweat Glucose Biosensor

Xiaoyang Xuan^{a, c}, Min Qian^{a, *}, Likun Pan^{b, *}, Ting Lu^b, Lu Han^b, Huangze Yu^b, Lijia Wan^b, Yueping Niu^{a, c}, Shangqing Gong^{a, c, *}

^a Department of Physics, School of Science, East China University of Science and Technology, Shanghai, 200237, People's Republic of China

*Corresponding author. E-mail address: mqian@ecust.edu.cn

^b Shanghai Key Laboratory of Magnetic Resonance, School of Physics and Electronic Science, East China Normal University, Shanghai, 200062, People's Republic of China

*Corresponding author. E-mail address: lkpan@phy.ecnu.edu.cn

^c Key Laboratory for Ultrafine Materials of Ministry of Education, Shanghai Engineering Research Center of Hierarchical Nanomaterials, School of Materials Science and Engineering, East China University of Science and Technology, Shanghai, 200237, People's Republic of China

*Corresponding author. E-mail address: sqgong@ecust.edu.cn

S1. Current Response and Scan Rate for Glucose Detection

CV curves of 0, 60, and 120 min Ni-MOFs in 0.1 M NaOH solutions with 0 or 100 μM glucose at various potential scan rates from 10 to 100 mV s^{-1} are shown in Fig. S1a and b, Fig. S1d and e, Fig. S1g and h, respectively. As shown in Fig. S1a, d and g, the well-defined oxidation peaks near 0.50 V and reduction peaks near 0.30 V in CV curves are ascribed to typical redox reactions between Ni ions and OH^- in alkaline solution. With increasing potential scan rate, the oxidation peak moves toward larger potential value, while the reduction peak shifts toward smaller potential value, which is ascribed to the hindered electron transfer process at electrode/electrolyte interface.¹ Similar phenomenon has also been observed in 0.1 M NaOH solution with 100 μM glucose for each sample, as shown in Fig. S1b, e and (h). The 60 min Ni-MOF exhibits the highest current densities both in 0.1 M NaOH solutions with 0 and 100 μM glucose as shown in Fig. S1d and e, in comparison with those of 0 and 120 min Ni-MOFs as shown in Fig. S1a and b, Fig. S1g and h.

The data in Fig. S1 has been further analyzed according to equation (S1), with derived results illustrated in Fig. S1c, f and i.

$$i = a v^b \quad (\text{S1})$$

where i is current density at a specific potential scan rate v obtained from CV curves, a and b are adjustable parameters. The dependence of increasing current density on increasing scan rate is presented by the b value according to equation (S1), and explained by the balance between diffusion and adsorption processes.² For reversible processes, $b = 0.5$ represents a diffusion-dominated electrochemical process, and $b =$

1 indicates an adsorption-dominated electrochemical process.^{3,4} As shown in Fig. S1c, f and i, without glucose, the b values of 0, 60, and 120 min Ni-MOFs are all close to 0.5, indicating that the oxidation process of Ni-MOF is based on the diffusion of OH^- , while with 100 μM glucose, the b values of 0, 60, and 120 min Ni-MOFs are all less than 0.5, which is related to a restricted kinetics process.⁵ The slopes of $\log(\text{scan rate})$ versus $\log(\text{current density})$ with and without glucose are different in Fig. S1c, f and i, where the two linear fitting lines intersects at a certain high scan rate between 60 and 100 mV s^{-1} , which means that a current gain can be obtained at lower sweep speeds ($< \sim 60 \text{ mV s}^{-1}$) while a current loss can be caused at higher sweep speeds in glucose solution, different with those in non-glucose solution. For this reason, we choose the potential scan rate of 20 mV s^{-1} in the following CV test.

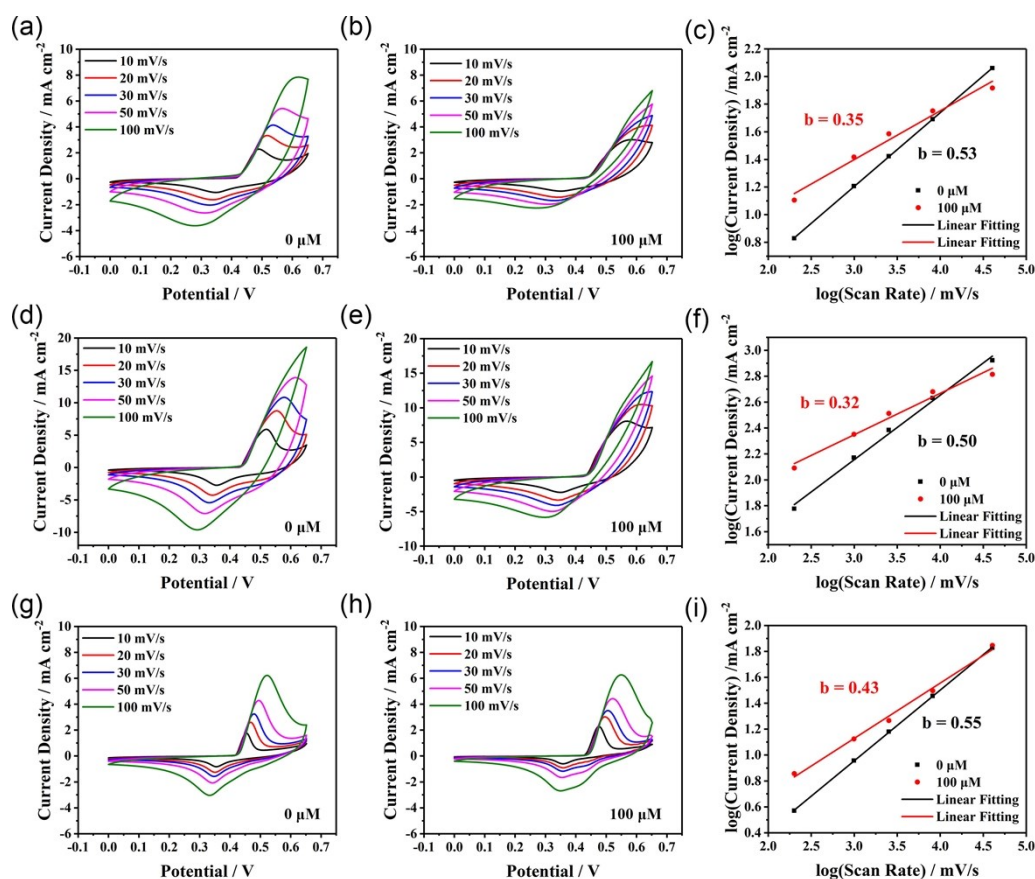


Fig. S1 CV curves of 0 min Ni-MOF in 0.1 M NaOH solutions (a) without glucose

and b with 100 μM glucose at various potential scan rates from 10 to 100 mV s^{-1} . (c) Linear analysis of peak current density and potential scan rate for 0 min Ni-MOF. CV curves of 60 min Ni-MOF in 0.1 M NaOH (d) without glucose and (e) with 100 μM glucose at various potential scan rates from 10 to 100 mV s^{-1} . (f) Linear analysis of peak current density and potential scan rate for 60 min Ni-MOF. CV curves of 120 min Ni-MOF in 0.1 M NaOH (g) without glucose and (h) with 100 μM glucose at various potential scan rates from 10 to 100 mV s^{-1} . (i) Linear analysis of peak current density and potential scan rate for 120 min Ni-MOF.

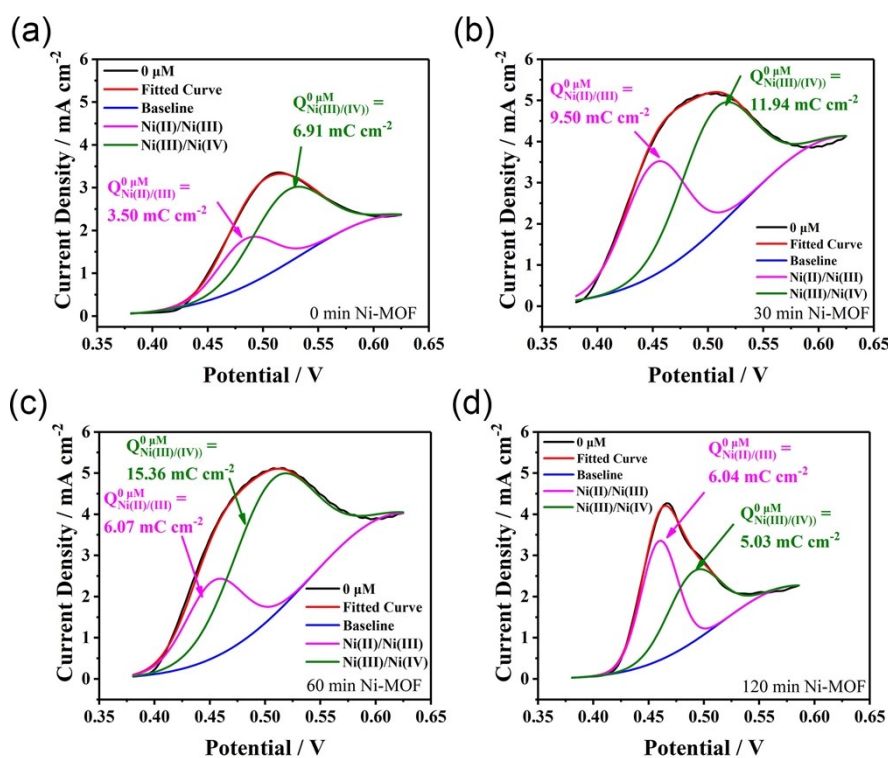


Fig. S2 CV peak separation of (a) 0 min, (b) 30 min, (c) 60 min, and (d) 120 min Ni MOF at 20 mV s^{-1} in 0.1 M NaOH solution without glucose.

S2. Calculation of Diffusion Coefficient D

The slopes of the fitted linear curves in Fig. 8b are proportional to the diffusion coefficients D. The diffusion coefficients can be obtained by simplifying equation (7)

into equation (S2).

$$\frac{I_t}{A} = n F D^{1/2} C \pi^{-1/2} t^{-1/2} \quad (\text{S2})$$

where the ordinate is the current density (A cm^{-2}), the slope S can be expressed as equation (S3), and the diffusion coefficient D can be obtained by simplifying equation (S3) into equation (S4).

$$S = n F D^{1/2} C \pi^{-1/2} \quad (\text{S3})$$

$$D = \frac{\pi S^2}{C^2 F^2 n^2} \quad (\text{S4})$$

where n is the number of electrons in the redox process ($n = 1$), F is 96485 C mol^{-1} . The bulk concentration C ($0.1\text{M} + 100 \mu\text{M}$) is $10.01 \times 10^{-5} \text{ mol cm}^{-3}$. Slope S is 4.92×10^{-3} , 6.69×10^{-3} and $5.59 \times 10^{-3} \text{ A cm}^{-2} \text{ s}^{-1}$ for 0, 60 and 120 min Ni-MOFs, respectively. The diffusion coefficient D of catalytic process can be calculated to be 8.15×10^{-7} , 1.51×10^{-6} and $1.04 \times 10^{-6} \text{ cm}^2 \text{ s}^{-1}$ for 0, 60 and 120 min Ni-MOFs, respectively.

S3. Calculation of Active Surface Area

The active surface area can be obtained by simplifying equation (8) into equation (S5).

$$A = \frac{I_p}{0.4463 \sqrt{\frac{C^2 D n^3 F^3 v}{RT}}} \quad (\text{S5})$$

In Fig. S1b, e and (h), the current density (electrode area = 0.07 cm^2) in 0.1 M NaOH and $100 \mu\text{M}$ glucose solution are 4.13 , 10.51 and 3.03 mA cm^{-2} for 0, 60 and 120 min Ni-MOFs at 20 mV s^{-1} , respectively. The values of current I_p are 2.92×10^{-4} , $7.43 \times$

10^{-4} , 2.14×10^{-4} A for 0, 60, and 120 min Ni-MOFs. The bulk concentration ($0.1 \text{ M} + 100 \text{ }\mu\text{M}$) equals to $10.01 \times 10^{-5} \text{ mol cm}^{-3}$. n is the number of electrons in the redox process ($n = 1$). F is 96485 C mol^{-1} . R is $8.314 \text{ J mol}^{-1} \text{ K}^{-1}$. T is 298.15 K . The CV scan rate ν is 0.02 V s^{-1} . D is 8.15×10^{-7} , 1.51×10^{-6} and $1.04 \times 10^{-6} \text{ cm}^2 \text{ s}^{-1}$ for 0, 60 and 120 min Ni-MOFs, respectively.

Therefore, we can roughly estimate the active surface area related to glucose detection performance of Ni-MOF electrode in 0.1 M NaOH solution with $100 \text{ }\mu\text{M}$ glucose to be 0.09 , 0.16 , and 0.06 cm^2 for 0, 60, and 120 min Ni-MOFs, respectively.

Table S1. Comparison of current response and linear range in glucose detection using 60 min Ni-MOF with other studies in the literatures.

Sample	Sweeping potential methods (such as cyclic voltammetry)		Fixed potential methods (such as chronoamperometry)		Reference
	Sensitivity / $\mu\text{A mM}^{-1} \text{ cm}^{-2}$	Linear Range/ μM	Sensitivity / $\mu\text{A mM}^{-1} \text{ cm}^{-2}$	Linear Range / μM	
Au nanowire array	728	500-14000	309.0	1000-10000	6
Au nano/Ti	1389	1000-15000	--	--	7
Ni-MOF nanobelts	--	--	1.54	1-500	8

Ni ^{II} MOF	--	--	585	40-500	9
Ni-MOF/carbon nanotubes	--	--	77.7	20-4400	10
NiFe-MOF/Ni	--	--	41950	2-1600	11
NiCo-MOF/Au	--	--	684	1-8000	12
60 min Ni- MOF	3297.10	0-400	3.03	0-2000	This work
60 min Ni- MOF	2260.77	400-1000	0.95	2000-3500	This work

References

1. M. S. Rahmanifar, H. Hesari, A. Noori, M. Y. Masoomi, A. Morsali and M. F. Mousavi, A dual Ni/Co-MOF-reduced graphene oxide nanocomposite as a high performance supercapacitor electrode material, *Electrochim. Acta*, 2018, **275**, 76-86.
2. S. K. Hassaninejaddarzi and M. Gholamiesfidvajani, Preparation of nanoporous nickel phosphate VSB-5 nanorods carbon paste electrode as glucose non-enzymatic sensor, *J. Porous Mater.*, 2017, **24**, 85-95.
3. Y. Shao, M. F. El-Kady, J. Sun, Y. Li, Q. Zhang, M. Zhu, H. Wang, B. Dunn and R. B. Kaner, Design and mechanisms of asymmetric supercapacitors, *Chem. Rev.*, 2018, **118**, 9233-9280.
4. S. K. Hassaninejaddarzi, Fabrication of a non-enzymatic Ni(II) loaded ZSM-5 nanozeolite and multi-walled carbon nanotubes paste electrode as a glucose

- electrochemical sensor, *RSC Adv.*, 2015, **5**, 105707-105718.
5. S. N. Azizi, S. Ghasemi and H. Yazdanisheldarrei, Synthesis of mesoporous silica (SBA-16) nanoparticles using silica extracted from stem cane ash and its application in electrocatalytic oxidation of methanol, *Int. J. Hydrogen Energy*, 2013, **38**, 12774-12785.
 6. S. Cherevko and C. H. Chung, Gold nanowire array electrode for non-enzymatic voltammetric and amperometric glucose detection, *Sens. Actuators B Chem.*, 2009, **142**, 216-223.
 7. Q. Yi and W. Yu, Electrocatalytic activity of a novel titanium-supported nanoporous gold catalyst for glucose oxidation, *Microchim. Acta*, 2009, **165**, 381-386.
 8. X. Xiao, S. Zheng, X. Li, G. Zhang, X. Guo, H. Xue and H. Pang, Facile synthesis of ultrathin Ni-MOF nanobelts for high-efficiency determination of glucose in human serum, *J. Mater. Chem. B*, 2017, **5**, 5234-5239.
 9. N. S. Lopa, M. M. Rahman, F. Ahmed, S. C. Sutradhar, T. Ryu and W. Kim, A Ni-based redox-active metal-organic framework for sensitive and non-enzymatic detection of glucose, *J. Electroanal. Chem.*, 2018, **822**, 43-49.
 10. F. Wang, X. Chen, L. Chen, J. Yang and Q. Wang, High-performance non-enzymatic glucose sensor by hierarchical flower-like nickel(II)-based MOF/carbon nanotubes composite, *Mater. Sci. Eng. C Mater. Biol. Appl.*, 2019, **96**, 41-50.
 11. L. Zhang, X. Ma, H. Liang, H. Lin and G. Zhao, A non-enzymatic glucose

sensor with enhanced anti-interference ability based on a MIL-53(NiFe) metal-organic framework, *J. Mater. Chem. B*, 2019, **7**, 7006-7013.

12. W. Li, S. Lv, Y. Wang, L. Zhang and X. Cui, Nanoporous gold induced vertically standing 2D NiCo bimetal-organic framework nanosheets for non-enzymatic glucose biosensing, *Sens. Actuators B Chem.*, 2019, **281**, 652-658.